Measurements of the Low Frequency Noise Properties of a 30 GHz High-Electron-Mobility-Transistor Amplifier

Norman Jarosik Lyman Page David Wilkinson
Ed Wollack

12 June 1993

Abstract

Low frequency noise parameters of a 30 GHz cryogenic HEMT amplifier have been measured with the input of the amplifier connected to a 15 K load. Significant excess low frequency noise has been observed and identified with gain fluctuations in the amplifier. The spectral density of these fluctuations grows to 1.5 times the high frequency value at 3.5 Hz and twice the high frequency value at 1.7 Hz. Strong correlation between output power fluctuations of the amplifier and drain current fluctuations of the transistors comprising the amplifier are observed. The existence of these correlations introduces the possibility of regressing some of the excess noise from the HEMT amplifier's output using the measured drain currents. This report is presented in fulfillment of JPL contract # 959556.

1 Introduction

Recently, major advances have been made in the noise performance and frequency range of cryogenic HEMT (High Electron Mobility Transistor) amplifiers. Their ruggedness, reliability, large bandwidths and modest cooling

requirements have made them the preferred front ends for low noise radiometry applications below 90 GHz. Most radiometers employ some form of Dicke switching in order to minimize the effects of systematic errors and long term drifts. The switching frequency is usually determined by two competing effects. In the case of radio telescopes the Dicke switching is often accomplished through the motion of a large optical element, therefore mechanical considerations favor a slow switching rate. The rate at which the switching is done must be fast enough that the time varying parameters of the radiometer do not change between switch positions. Choosing the best compromise between these two competing requirements necessitates knowledge of the stability characteristics of all the radiometer components. The amplifiers studied in this report are so new that no thorough investigations of their stability characteristics have been made to date. This work attempts not only to characterize the device under study, a cryogenic 25–35 GHz NRAO HEMT amplifier, but also to develop the techniques required to perform such measurements quickly and reliably, substantially reducing systematic errors introduced by the associated test equipment.

2 Technique

The major obstacle in characterizing the stability of the HEMT amplifiers is that the other components used in performing the measurement typically have stabilities comparable to or worse than the HEMT amplifier under test. The resultant measurements therefore reflect not only the variability of the parameters of the amplifier under test, but also the variability of the components comprising the test setup. One way to overcome this problem is to carefully measure the relevant parameters of all the components of the test set-up, and then attempt to de-convolve their effects from the data. However, this technique requires the relevant parameters of the components of the test system to remain constant both from day to day and in the different configurations required to measure the various parameters. Such difficulties, and the inherent errors introduced by attempting the de-convolution of the data make this technique problematic.

The approach used here is fundamentally different than that described above in that it makes no assumptions about the stability or repeatability of the characteristics of most of the components of the test setup. Rather,

it merely requires that the fluctuations inherent in two different sets of test components be uncorrelated. A simplified description of this technique follows.

Assume that an amplifier under test is connected as shown in Figure 1a, with its input attached to a temperature stabilized cold load. Let the time dependent output power of the HEMT amplifier, $H(t)$, be given by

$$H(t) = \overline{H} + \delta H(t), \tag{1}$$

$$< \delta H(t) > \equiv 0, \tag{2}$$

where both the effects of noise temperature fluctuation and gain fluctuations of the HEMT are included in the term $\delta H(t)$, $\overline{H}$ denotes the mean value of the output power of the HEMT amplifier, and <> denotes an average over a time long compared to the time scale of the fluctuations of interest. The output of the HEMT amplifier is then divided, amplified and detected by two (nominally) identical amplifier channels. The detected total power signals from the two outputs are described by

$$P_1(t) = H(t)G_1(t) = \left[\overline{H} + \delta H(t)\right]\left[(\overline{G_1} + \delta G_1(t)\right], \tag{3}$$

$$P_2(t) = H(t)G_2(t) = \left[\overline{H} + \delta H(t)\right]\left[(\overline{G_2} + \delta G_2(t)\right]. \tag{4}$$

Here $\delta G_1(t)$ and $\delta G_2(t)$ represent the time varying components of the gains of room temperature amplifiers, and $\overline{G_1}$ and $\overline{G_2}$ are the mean gains of these amplifiers. (For simplicity the room temperature amplifier chains are assumed to have only gain fluctuations. This assumption is not neccesary, and is made here only for simplicity. The only crucial assumption is that the time varying parameters of the two room temperature amplifier chains be uncorrelated.) Taking the power spectrum of either $P_1(t)$ or $P_2(t)$ characterizes the stability of each radiometer channel as a whole, but sheds little light on which components (HEMTs, room temperature amplifiers or detectors) exhibit the variability. In order to extract the HEMT characteristics the cross-correlation of $P_1(t)$ and $P_2(t)$ is formed:

$$\text{Corr}(T) \equiv \int (P_1(T-t) \cdot P_2(t) dt, \tag{5}$$

$$\text{Corr}(T) = \int \left[\overline{H} + \delta H(t)\right]\left[\overline{G} + \delta G_1(t)\right] \cdot \tag{6}$$

$$\left[\overline{H} + \delta H(T-t)\right]\left[\overline{G} + \delta G_2(T-t)\right] dt. \tag{7}$$

Next, Corr(T) is ensemble averaged, recalling that the means of all the fluctuating components are defined as zero, and that all cross terms of δG_1, δG_2 and δH vanish as a result of their statistical independence. The only terms which survive the averaging are

$$< \mathrm{Corr}(T) >= \overline{H}^2\overline{G}^2 + \overline{G}^2 < \int [\delta H(T-t)\delta H(t)]dt >, \qquad (8)$$

the second of which is proportional to the auto-correlation function of the fluctuating component of the power output of the HEMT amplifier. This auto-correlation function can be converted to the power spectrum of the fluctuations by a Fourier transform. The effects of the variability of the parameters of the room temperature components are eliminated in the limit in which those parameters are uncorrelated and average to zero; the variablility is manifest as additional statistical noise on the measured correlation functions and power spectra. In general obtaining power spectra in this manner only picks out components which are correlated in the two data streams and can therefore be used to search for correlations between any time varying parameters in the radiometer. This proves to be a very powerful technique and has been used extensively in this study.

3 Apparatus and Data Collection

The system used to make the measurements (Figure 1b) consists of both cryogenic and room temperature components. The cryogenic components are two HEMT amplifiers, an orthomode coupler and a variable temperature load. The HEMT amplifiers were designed and constructed by NRAO under the directon of Marian Pospieszalksi. Each amplifer comes paired with a circuit board which sets the operating point of each of the four transistors comprising the amplifier. These amplifiers have a gain of about 30 dB from 25–35 GHz, and a mean noise temperature of about 40 K when operated at a temperature of 15 K. The cryogenic components are located inside a vacuum-insulated dewar which is cooled by a mechanical refrigerator. The refrigerator is capable of cooling the cold plate, to which the amplifier and orthomode coupler are attached, to about 10 K. The amplifier body has a heater resistor and a GaAs cryogenic thermometer attached to it. The inputs of the two HEMT amplifiers are connected to the two single polarization ports

of the orthomode transducer, and the dual polarization port is attached to an unpolarized cold load. The cold load consists of an Eccosorb cone inside a round stainless steel waveguide. This conical piece of Eccosorb is connected to the cold plate through a weak thermal link, and is outfitted with a non-inductive heater and a silicon diode temperature sensor. A Lakeshore Cryotronics temperature regulator is used to regulate the load temperature. The outputs of the two HEMT amplifiers are brought to a room temperature port on the dewar by two sections of stainless steel waveguide which have been gold plated on their interiors to minimize losses. The room temperature end of each waveguide has a broadband isolator attached to minimize standing waves from reflections from the inputs of the room temperature amplifiers.

The room temperature part of the system consists of two nominally identical channels, designated A and B. Each channel consists of a broadband waveguide amplifier, and a frequency triplexer constructed from circulators and waveguide bandpass filters. The different frequency bands are designated 1, 2 and 3, and have nominal pass bands of 26–29, 29–32 and 32–35 GHz, respectively. A diode detector is located at the output of each filter bank, and its output is fed into the data collection system after amplification by low noise amplifiers.

Each of the six channels of the data collection system (designated 1A, 2A, 3A, 1B, 2B, and 3B, with the number corresponding to the frequency band and the letter indicating the radiometer channel) consists of a Bessel anti-alias filter, a voltage to frequency converter and a counter. The contents of the counter are read out and the counter re-zeroed at a rate of 62.5 Hz. The bandpasses of all the six channels of the data collection system are nearly identical. Each bandpass was characterized by applying a digitally synthesized white noise source to the input of each channel. The resulting response curve was empirically fit to an analytic form, and this form used to correct all the resulting spectra. Figure 2 shows responses of each channel after applying this rolloff correction.

4 Measurements and Results

The room temperature amplifier chains were connected to the dewar output waveguides in several different configurations, depending on the measurement being made. Each configuration is described below, along with the results

obtained from each.

4.1 Independent Channels

The first configuration employed was the same as shown in Figure 1b, in which the two channels are independent of one another, since the only components in common are the orthomode coupler and the cold load. The spectral noise density on the output of the six detectors as a function of frequency is shown in Figure 3. These spectra were obtained as follows: first the time stream of data from the diode detectors representing the instantaneous output power of the radiometer was divided into blocks consisting of 1024 consecutive samples. After removal of the mean of each block, the block's auto-correlation function was formed. These auto-correlation functions were averaged, then Fourier transformed, yielding a power spectrum of the fluctuations of the output power of the radiometer. It should be noted that the power spectra calculated this way are not positive definite; in the situation where the correlated signal in the two time streams is small compared to the random noise, negative values can result. The figures show the square-root of the magnitude power spectral density (dimensions of $K/\sqrt{Hz}$) at each frequency and are displayed as negative if the value of the calculated power spectrum is negative. Each spectrum is normalized so that the mean value between 25 and 31.25 Hz (the Nyquist frequency) equals unity. This normalization compensates for the different losses, gains and responsivities associated with the different channels and bands, and facilitates comparison of different spectra. All the spectra in Figure 3 look very similar, and reflect the stability of the radiometer as a whole, but lend no insight as to the relative contributions of the various components to the overall radiometer stability. There is clearly an excess of noise at low frequncies, though from these data alone the source of this excess is not certain.

In this configuration, one expects the outputs of the various channels to be uncorrelated, aside from temperature fluctuations of the load. (Losses in the orthomode junction are small enough to be ignored.) Figure 4 shows the results: all possible cross-correlations of the signals from channels A and B. The normalization for each of these cross-correlations is determined by using the appropriate combination of normalization constants derived from the auto-correlation of the two individual channels involved. For example, the normalization applied to the cross-correlation of channels 1A and 2B is

$\sqrt{N_{1A}N_{2B}}$, where N_{1A} and N_{2B} are the normalization constants derived from auto-correlations of channels 1A and 2B respectively. For all combinations there is no significant correlation between the channels, apart from a slight upturn at very low frequency. These spectra therefore set a limit on the temperature stability of the cold load. Had there been significant temperature fluctuations of the cold load they would have been correlated for all combinations of channels.

Figure 5 shows cross-correlations between different frequency bands within a radiometer channel. Here very significant correlations are evident. The fact that all these spectra have the same shape and amplitude seems to indicate that the output power of each radiometer channel is varying as a whole (i.e., equally and coherently across the entire RF bandwidth of the amplifier). Since the previous measurements precluded the possibility of variations in the emission from the cold load at this level, these fluctuations must be inherent in the radiometer itself. Figure 6 summarizes these results by plotting the autocorrelations for each radiometer channel and the frequency band to frequency band cross-correlations for each channel on the same scale.

4.2 Noise Source Measurements

These correlations between different frequency bands within a channel could have their source either in the HEMT or the room temperature amplifier. In order to investigate these correlations further the radiometer was reconfigured as shown in Figure 7. In this arrangement the output of a broadband noise tube is divided and fed into both room temperature channels. Figure 8 shows the power spectra of the six radiometer channels. Again they are all normalized to unity between 25 and 31.25 Hz. All the spectra are very similar and seem to have a slightly sharper knee at low frequency than those obtained with the HEMTs operating. Channel 2A has a noticeably softer knee than the other five channels. This has been traced to a detector diode with excessive low frequency noise.

Figure 9 shows the band-band cross-correlations in this configuration. Ideally one expects the signals in different frequency bands and different channels to be uncorrelated, apart from fluctuations in the output power of the noise tube. This behavior is exhibited by the combinations 2A–1B, 3A–1B, 1A–3B and 2A–3B. One does expect correlations between the outputs of the two amplifier channels when correlating the same frequency band, since

both radiometer channels are looking at the same source, and, due to the statistical nature of the source, there are intrinsic fluctuations in its output power. This behavior can be seen in cross-correlations 1A–1B, 2A–2B, and 3A–3B. The flat character of these spectra reflects the stability of the noise tube output power, showing only a slight increase over white noise at very low frequencies. The reason that a similar effect is not seen with the radiometer in the previous configurations is that in the previous configuration the two radiometer channels were looking at two different polarizations of radiation emitted by the cold load, the fluctuations of which are uncorrelated aside from macroscopic temperature variations of the load. The fact that the combinations 1A–2B and 3A–2B show some degree of correlation is a result of the fact that the freqency bands in the two channels for these combinations overlap slightly, due to different filter bandpasses in the triplexers.

Figure 10 shows the band to band correlations within the same radiometer channel measured with the noise tube installed. Again significant correlations occur, indicating that the room temperature amplifiers have significant gain variation occuring coherently across their entire RF bandwidths. Figure 11 shows the spectrum of each band within a channel and the band to band correlations within a channel on the same axis. Note that the band to band correlations are somewhat weaker than those measured with the HEMTs operating, suggesting that some of that observed correlation has its origin in the HEMTs.

4.3 HEMT Correlations

In order to directly measure the HEMT parameters, the radiometer was reconfigured as shown in Figure 12, where the output power from the HEMT is divided and then amplified by the two separate channels. Figure 13 shows the spectra of each of the channels individually, while Figure 14 shows the cross-correlations between channels. The small peaks evident in the 3A and 3B channels of Figure 13 arise from a 1.2 Hz oscillation of the physical temperature of the HEMT amplifier produced by the mechanical refrigerator. The combinations 1A–1B, 2A–2B and 3A–3B are the spectra of the output power of the HEMTs, with very little contamination from any of the other radiometer components. Since all these plots are time-averaged cross-correlations between the different room temperature channels, the effects of instabilities in the room temperature components are averaged out. The fact

that combinations 1A–1B, 2A–2B and 3A–3B level out at a higher value than the other combinations again is a reflection of the fact that there are intrinsic statistical fluctuations of the noise power on the output of the HEMT. Since these statistical fluctuations are uncorrelated between frequency bands, ideally one expects the other combinations to be uncorrelated and average to zero (aside from the filter overlap problems associated with combinations 1A–2B and 3A–2B as evidenced in the noise tube measurements). The fact that these other combinations are correlated and have nearly identical amplitudes and shapes strongly suggests that whatever instabilities are causing these correlations occur uniformly across the entire RF bandwidth of the HEMT amplifier.

4.4 Gain-Drain Current Correlations

As mentioned previously, the HEMT amplifiers used in this study were supplied with room temperature circuit boards which contain circuitry used to maintain the transistors in the amplifiers at their proper operating points. It was observed that while the drain voltage and current monitor outputs of these circuit boards were stable, significant low frequency (.05–10 Hz) noise appeared on the gate voltage output. In order to identify the source of these fluctuations, a simple passive bias circuit was constructed from resistors, potentiometers and capacitors, and adjusted so as to put the transistors at the same operating points as those set by the original circuit boards. In this configuration the gate voltage of (each) transistor was observed to be very stable, but the drain voltage exhibited low frequency noise, indicating a variation in the source-drain current in the transistor, and therefore in the I-V characteristic of the transistor. These two seemingly contradictory observations can be reconciled when the nature of the circuit on the NRAO-supplied bias circuit board is considered. These circuit boards are designed to maintain a constant drain voltage and drain current on each transistor in the HEMT amplifier. For each transistor there are two servo loops. One maintains the drain voltage of the transistor at a preset value, while the other measures the drain current and adjusts the gate voltage of the transistor in order to hold the drain current constant. Therefore fluctuations in the I-V characterisitics of the transistor will be converted into gate voltage fluctuations by these servo loops, since the drain voltage and current are required to remain constant. In order to rule out the possibility that these fluctuations

in drain current (or gate voltage) were caused by a common source, such as a power supply instability or faulty ground lead, cross-correlations between drain voltages of the different transistors were formed. No correlations between drain voltage fluctuations were found when using the passive bias circuits, nor were any found between gate voltages when using the active bias circuits. Taken altogether, the above observations indicate that *the sources of the fluctuations are the individual transistors in the HEMT amplifier.* In addition, spectra of the power outputs of the HEMT amplifiers were obtained using the cross-correlation technique. No differences were observed between spectra obtained with the two different bias circuits.

Having determined that these fluctuations originate as variability in the transistors themselves as opposed to instabilities in the bias circuitry, the question arises as to whether the fluctuations are related to fluctuations in the amplifiers' output power. In order to determine this, four of the data collection channels previously connected to detectors 2A, 2B, 3A, and 3B were used to monitor the drain voltages of the four transistors in the HEMT amplifier, biased using the passive bias circuits. Figure 15 shows the power spectra of channels 1A and 1B along with the spectra of the voltage fluctuations of the drain voltages of the four transistors. Again all the spectra are normalized so that their average value from 25–31.25 Hz is unity. To test for correlations between these fluctuations and the output power of the HEMT, cross-correlations between these drain voltages and the detected power were obtained, and are shown in Figure 16. In all cases very significant correlations between the drain voltage and the detected output power are observed. Similar results were obtained using the NRAO-supplied bias circuit board and monitoring the gate voltages of the transistors. The fact that the magnitude of the correlations is roughly constant for the four different transistors indicates that *the observed drain voltage fluctuations are correlated to gain changes rather than noise temperature changes.* Had they been correlated to noise temperature changes, one would expect the correlations to be smaller for the transistors later in the amplifier chain, since the noise added by each successive gain stage is a smaller fraction of the overall system noise temperature.

These measurements were repeated with the physical temperature of the amplifier at 12, 15 and 20 K, with no effect on any of the observed spectra. It was noted, however, that the temperature of the body of the HEMT amplifier varies 70 mK p-p coherently with the cycling of the mechanical refrigerator.

The frequency of this oscillation is very stable at 1.2 Hz. The fact that no strong 1.2 Hz line is observed in any of the obtained spectra indicates that the amplifier's parameters are nearly temperature independent. A final set of measurements were made with the LEDs (light emitting diodes which illuminate the transistors) switched off. These data are presented in Figure 17. There is a small improvement in stability at frequencies below $\approx$ 10 Hz when the LEDs are switched off. This improvement occurred immediately after the LEDs were extinguished, and no further changes were observed during the subsequent 12 hours.

5 Summary and Conclusions

Accurate measurements of the stability characteristics of a 25–35 GHz HEMT amplifier have been obtained and are summarized in Figure 18. These plots give the spectral density of fluctuations of the power at the output port of the HEMT amplifier obtained with the amplifier's input attached to a 15 K temperature-regulated load. These spectra were obtained from the 1A–1B, 2A–2B and 3A–3B cross-correlations using the radiometer as configured in Figure 12, and have been normalized to have a mean value of unity above 25 Hz. Table 1 contains data from the 1A–1B curve in tabular form. Measurements of the stability of the emission from the load indicate that temperature fluctuations of the load have a negligible contribution to these spectra, and the use of the cross-correlation technique has effectively eliminated sensitivity to fluctuations in the room temperature components. These spectra are substantially worse than expected, based on our experience with L-band cryogenic NRAO HEMT amplifiers. The reason for this difference is not now known, and is clearly of interest. It appears that most of the variability is characterized by the gain of the amplifier shifting uniformly across its entire RF bandwidth, with these variations being accompanied by changes in the drain currents of the individual transistors comprising the amplifier. The fact that these correlations occur raises the possibility of using the measured drain currents to regress some of the variability out of the data stream. The stability of the room temperature amplifiers in the set-up is comparable to that of the cryogenic HEMT, and in fact the nature of their fluctuations appears to be similar, occurring uniformly across the entire RF bandwidth of each amplifier. Since these amplifiers do not allow access to the individual drain

currents, it is not known whether these fluctuations are also accompanied by drain current variations.

Future efforts will be directed towards both understanding the source of these fluctuations and finding ways to minimize their effects on amplifier performance.

This work has been supported by JPL contract # 959556 and NSF grant NAGW-2801. The HEMT amplifers were provided on loan from the NRAO Electronic Division, Charlottesville, VA.

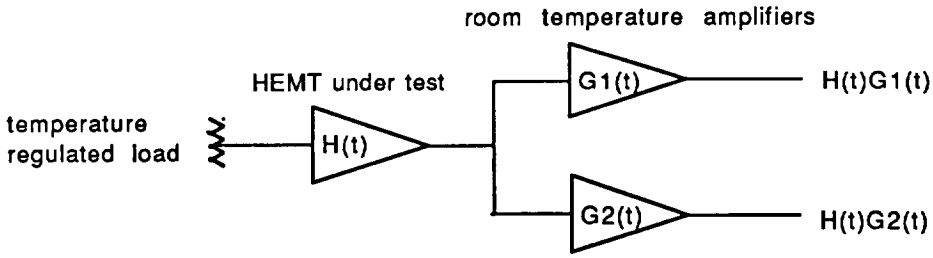

Figure 1a

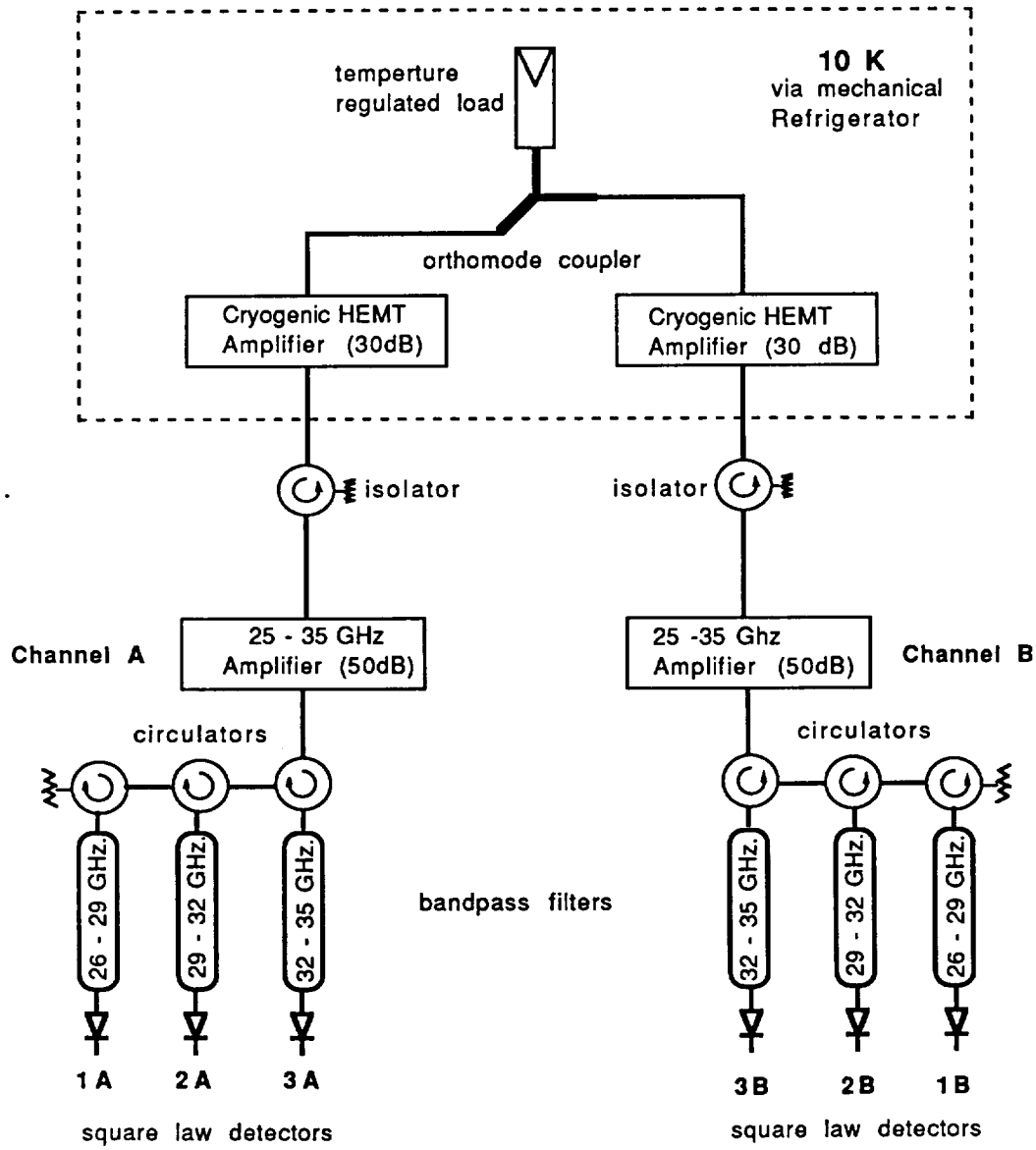

Figure 1b

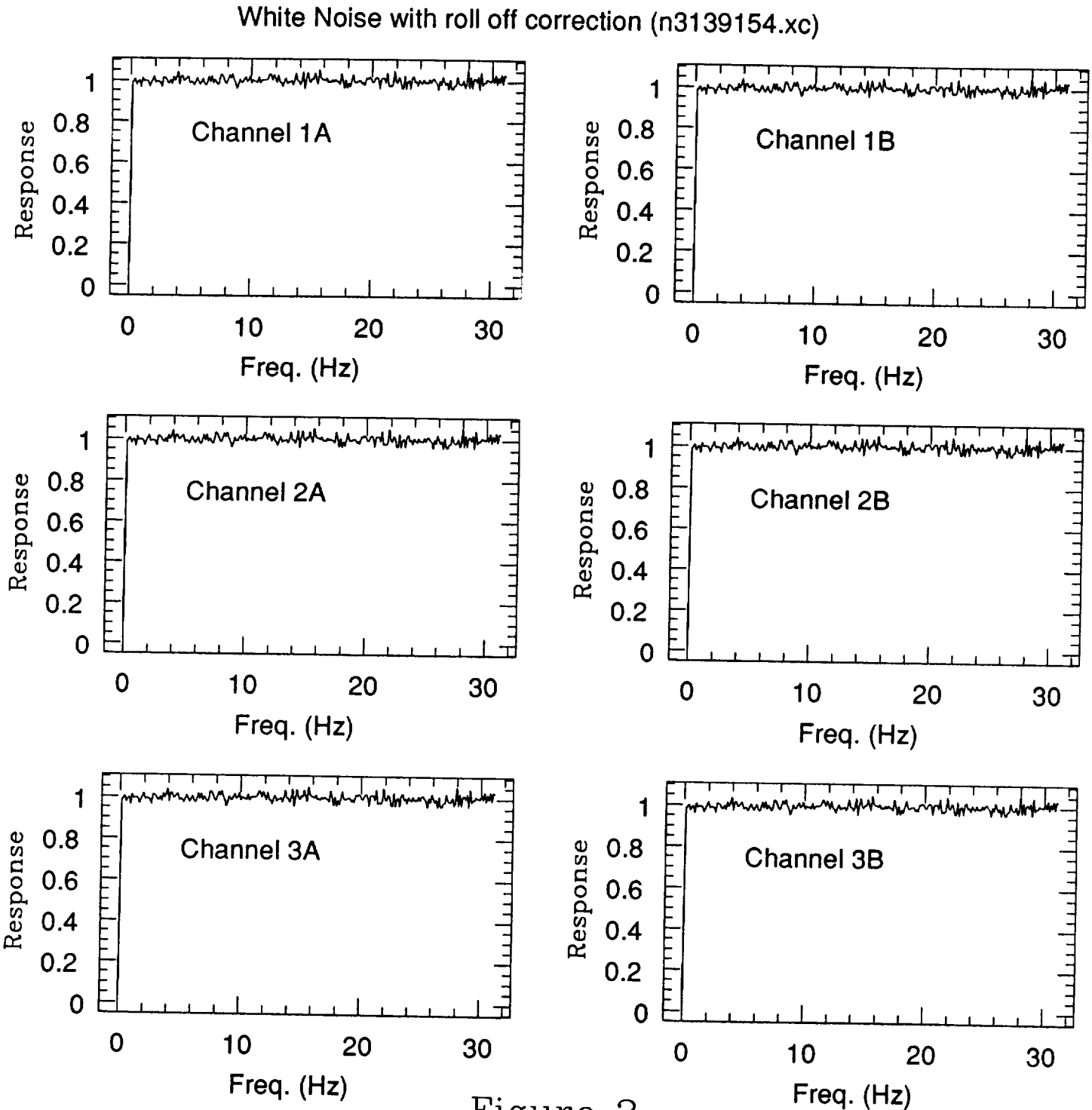
White Noise with roll off correction (n3139154.xc)
Channel 1A
Channel 1B
Channel 2A
Channel 2B
Channel 3A
Channel 3B
Response
Freq. (Hz)
0
0.2
0.4
0.6
0.8
1
0
10
20
30

Figure 2

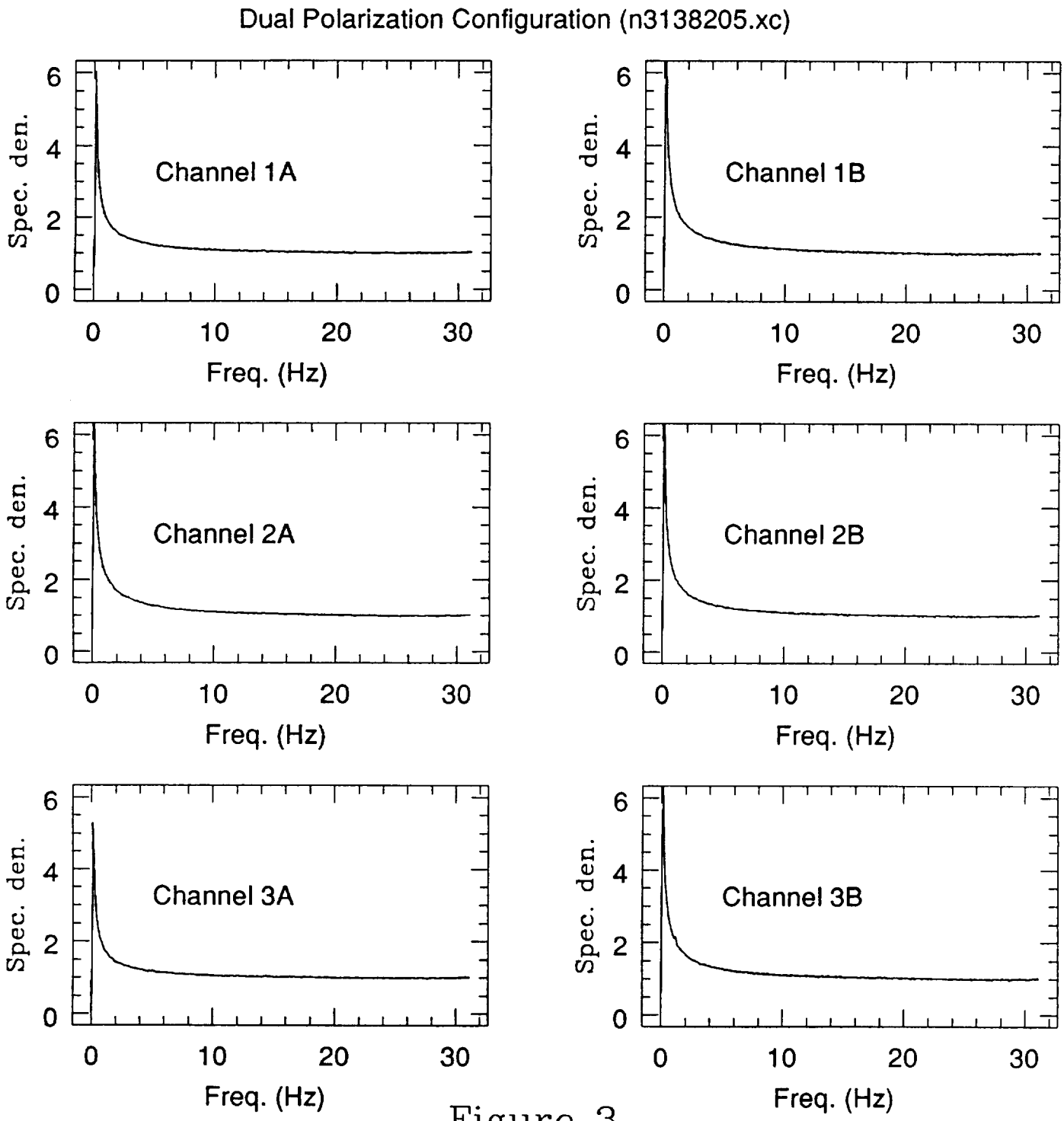
Dual Polarization Configuration (n3138205.xc)
Channel 1A
Channel 1B
Channel 2A
Channel 2B
Channel 3A
Channel 3B
Spec. den.
Freq. (Hz)
0
2
4
6
0
10
20
30

Figure 3

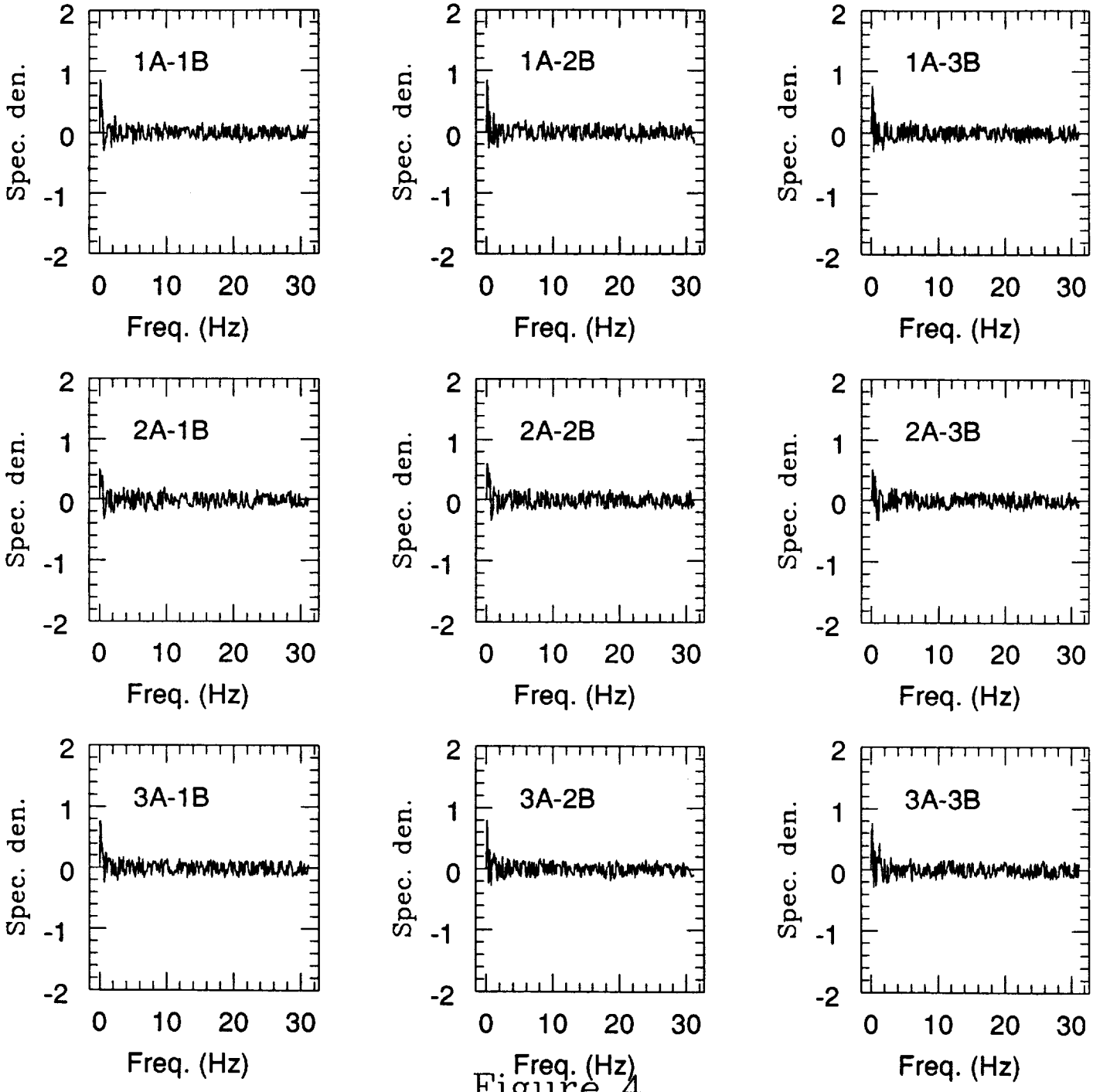
Dual Polarization Configuration (n3138205.xc)
1A-1B
1A-2B
1A-3B
2A-1B
2A-2B
2A-3B
3A-1B
3A-2B
3A-3B
Spec. den.
Freq. (Hz)
2
1
0
-1
-2
0
10
20
30

Figure 4

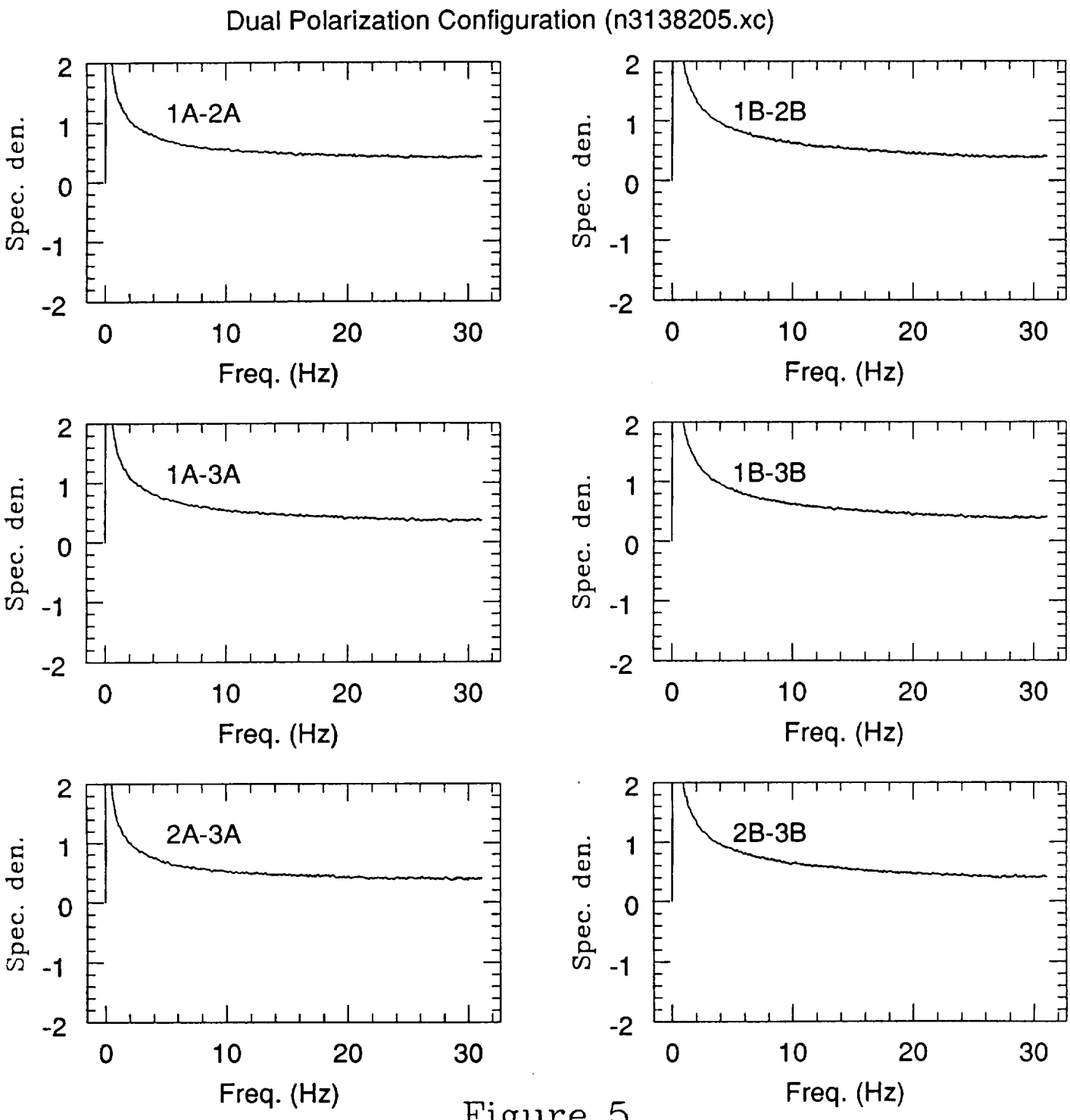
Dual Polarization Configuration (n3138205.xc)
1A-2A
1B-2B
1A-3A
1B-3B
2A-3A
2B-3B
Spec. den.
Freq. (Hz)
2
1
0
-1
-2
0
10
20
30

Figure 5

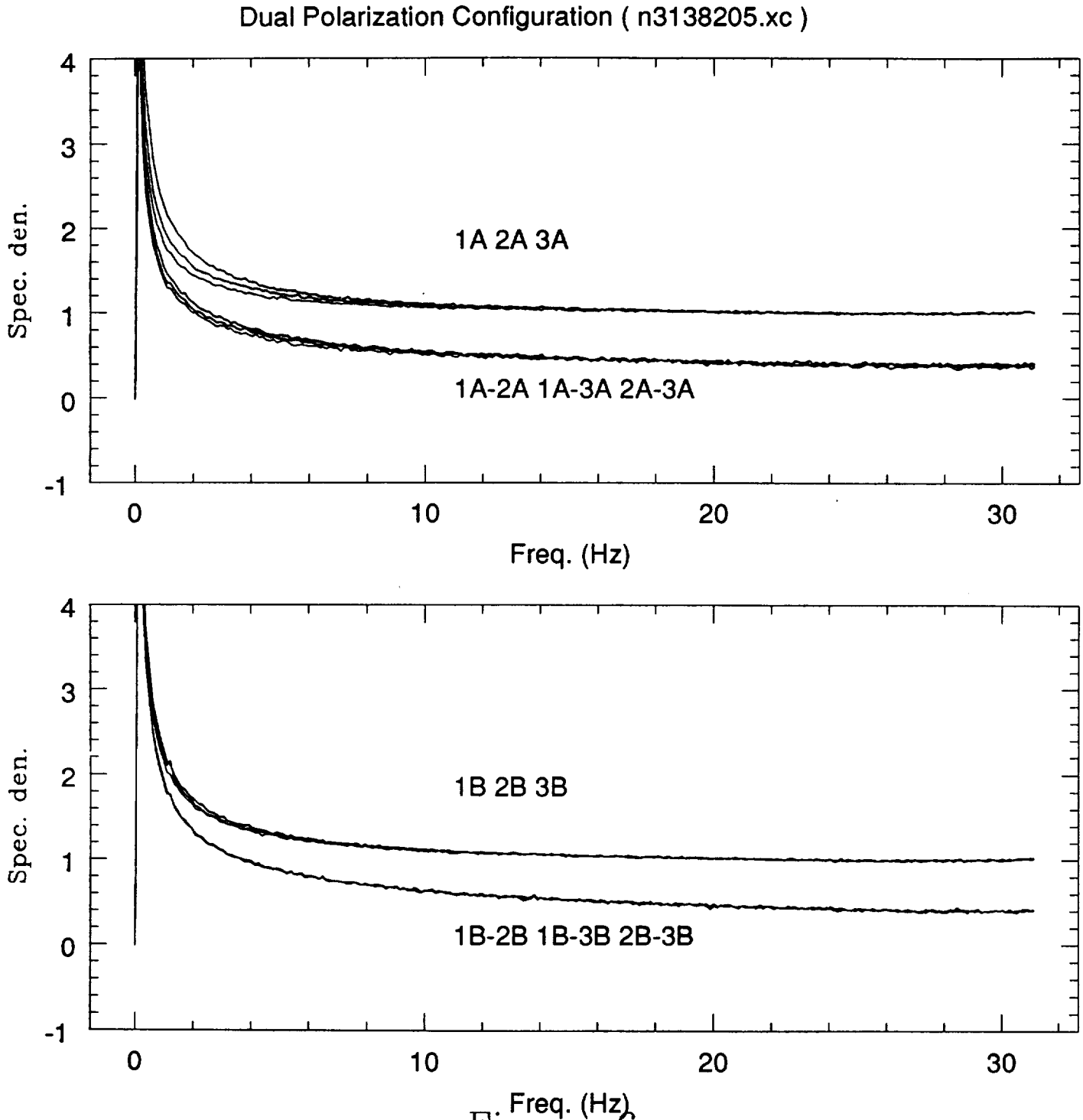
Dual Polarization Configuration (n3138205.xc)
Spec. den.
4
3
2
1
0
-1
1A 2A 3A
1A-2A 1A-3A 2A-3A
0
10
20
30
Freq. (Hz)
Spec. den.
4
3
2
1
0
-1
1B 2B 3B
1B-2B 1B-3B 2B-3B
0
10
20
30
Freq. (Hz)

Figure 6

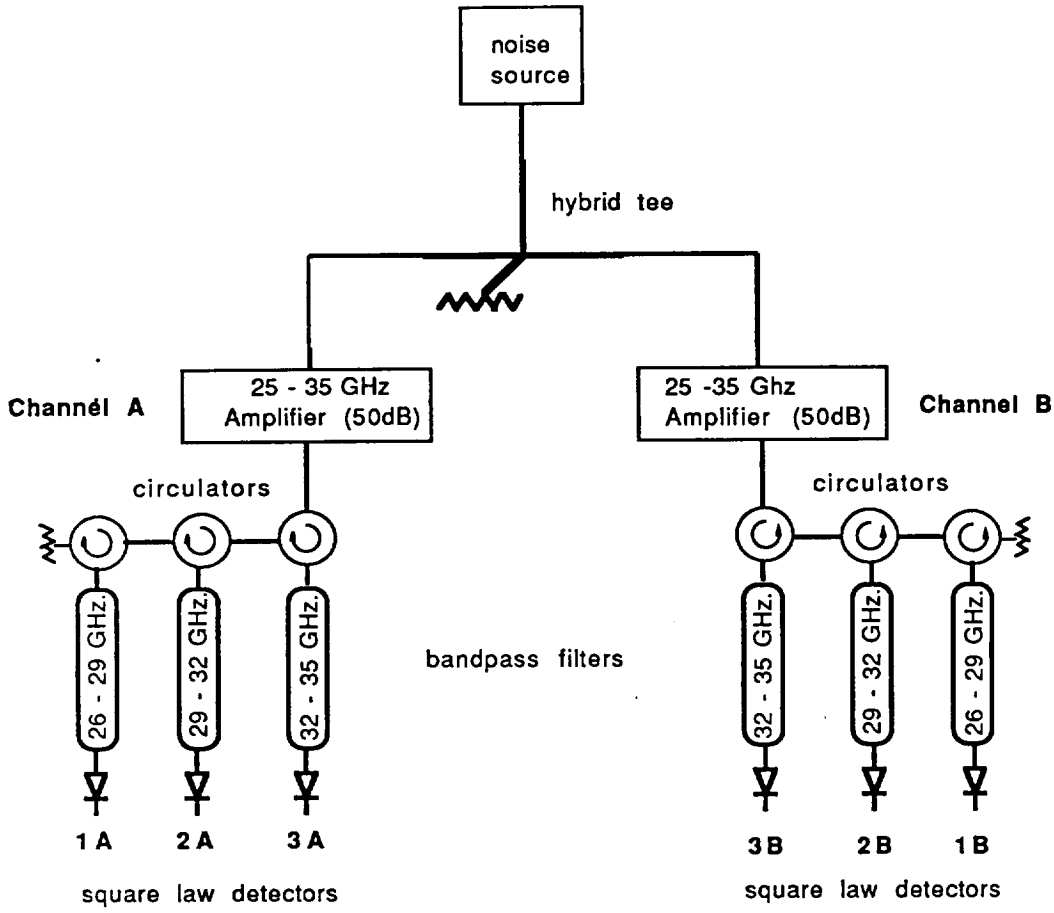
noise source
hybrid tee
Channel A
25 - 35 GHz Amplifier (50dB)
25 -35 Ghz Amplifier (50dB)
Channel B
circulators
circulators
26 - 29 GHz.
29 - 32 GHz.
32 - 35 GHz.
bandpass filters
32 - 35 GHz.
29 - 32 GHz.
26 - 29 GHz.
1 A
2 A
3 A
3 B
2 B
1 B
square law detectors
square law detectors

Figure 7

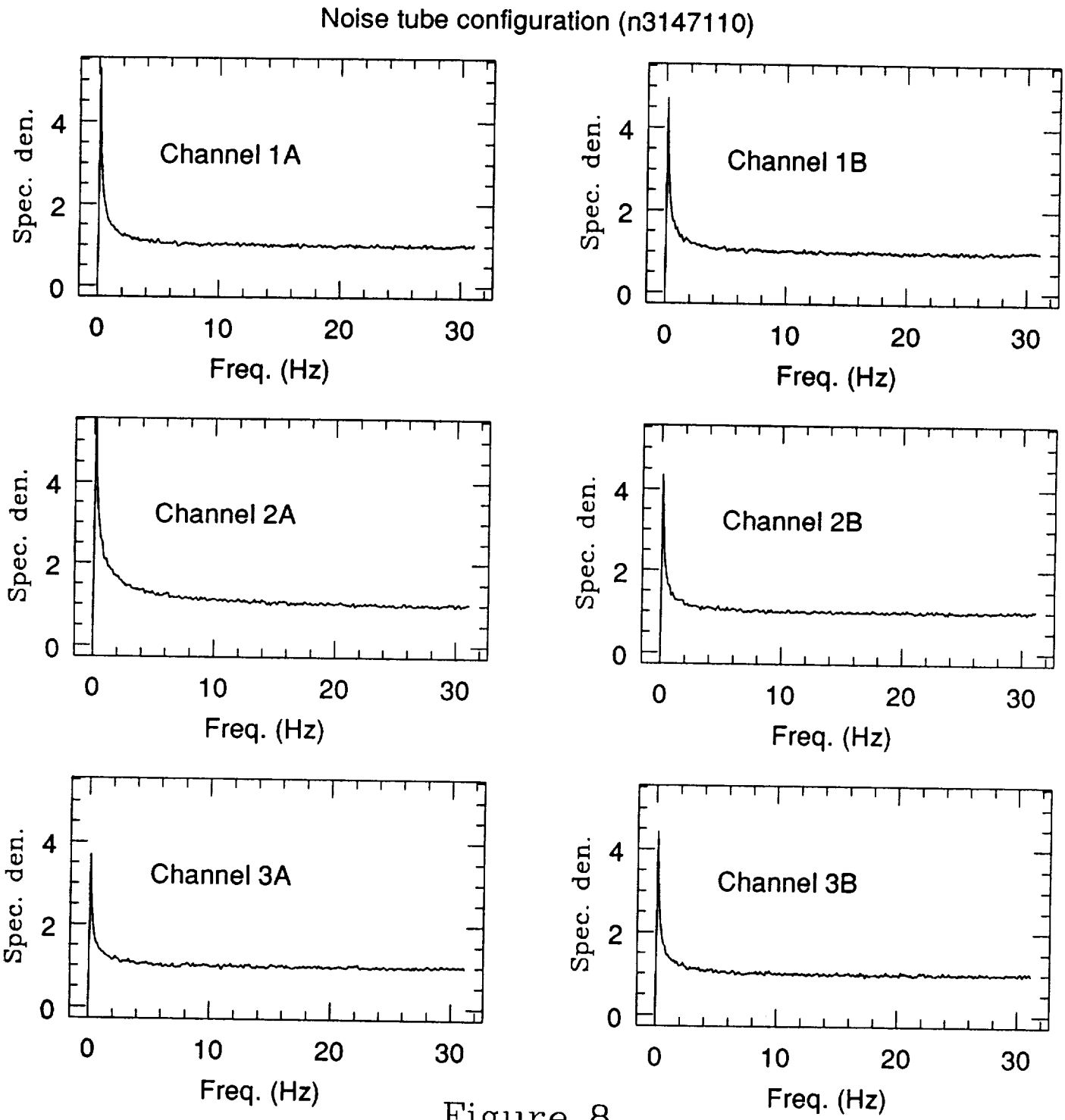
Noise tube configuration (n3147110)
Channel 1A
Channel 1B
Channel 2A
Channel 2B
Channel 3A
Channel 3B
Spec. den.
Freq. (Hz)
0
2
4
10
20
30

Figure 8

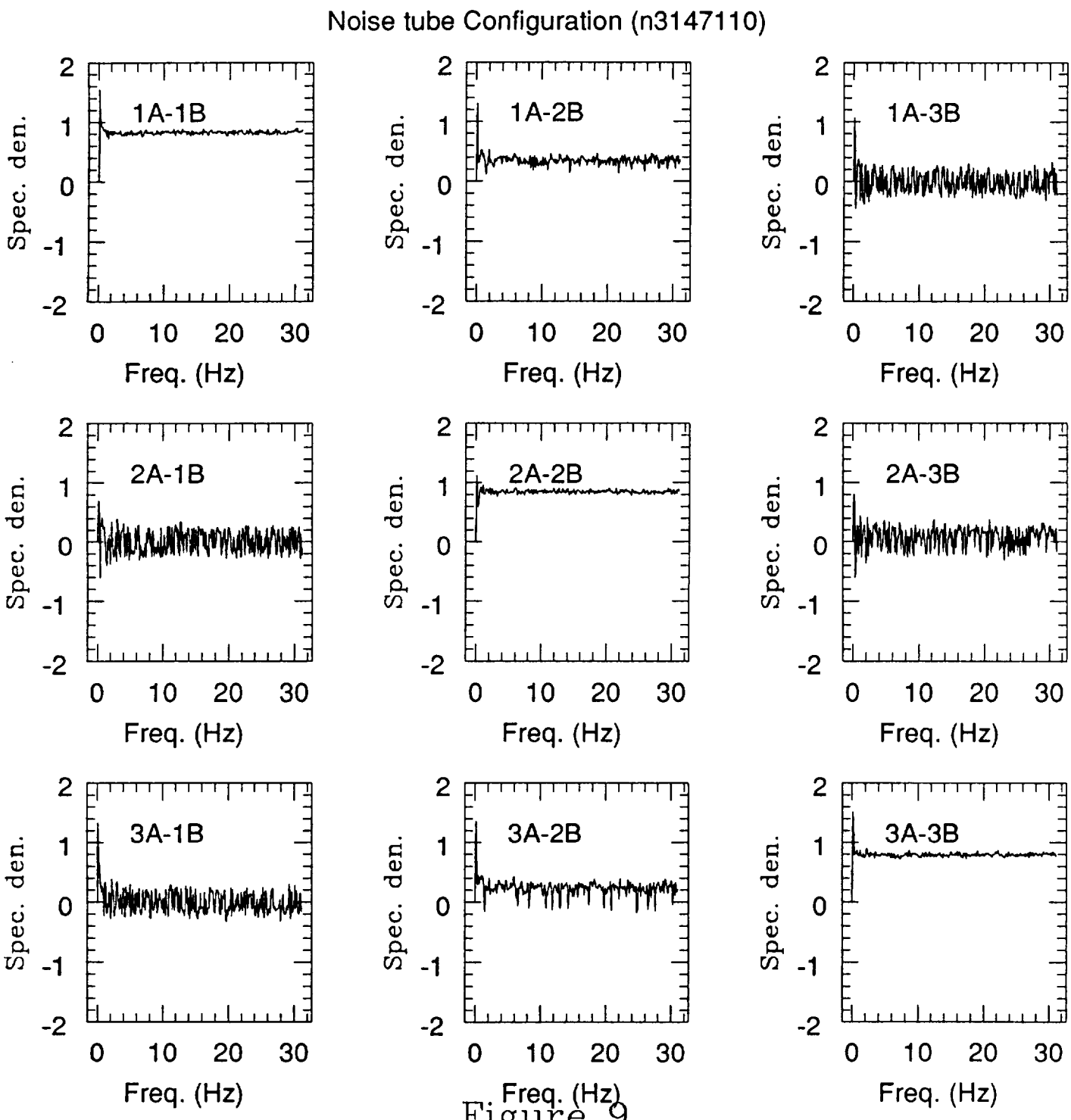
Noise tube Configuration (n3147110)
1A-1B
1A-2B
1A-3B
2A-1B
2A-2B
2A-3B
3A-1B
3A-2B
3A-3B
Spec. den.
Freq. (Hz)
2
1
0
-1
-2
0
10
20
30

Figure 9

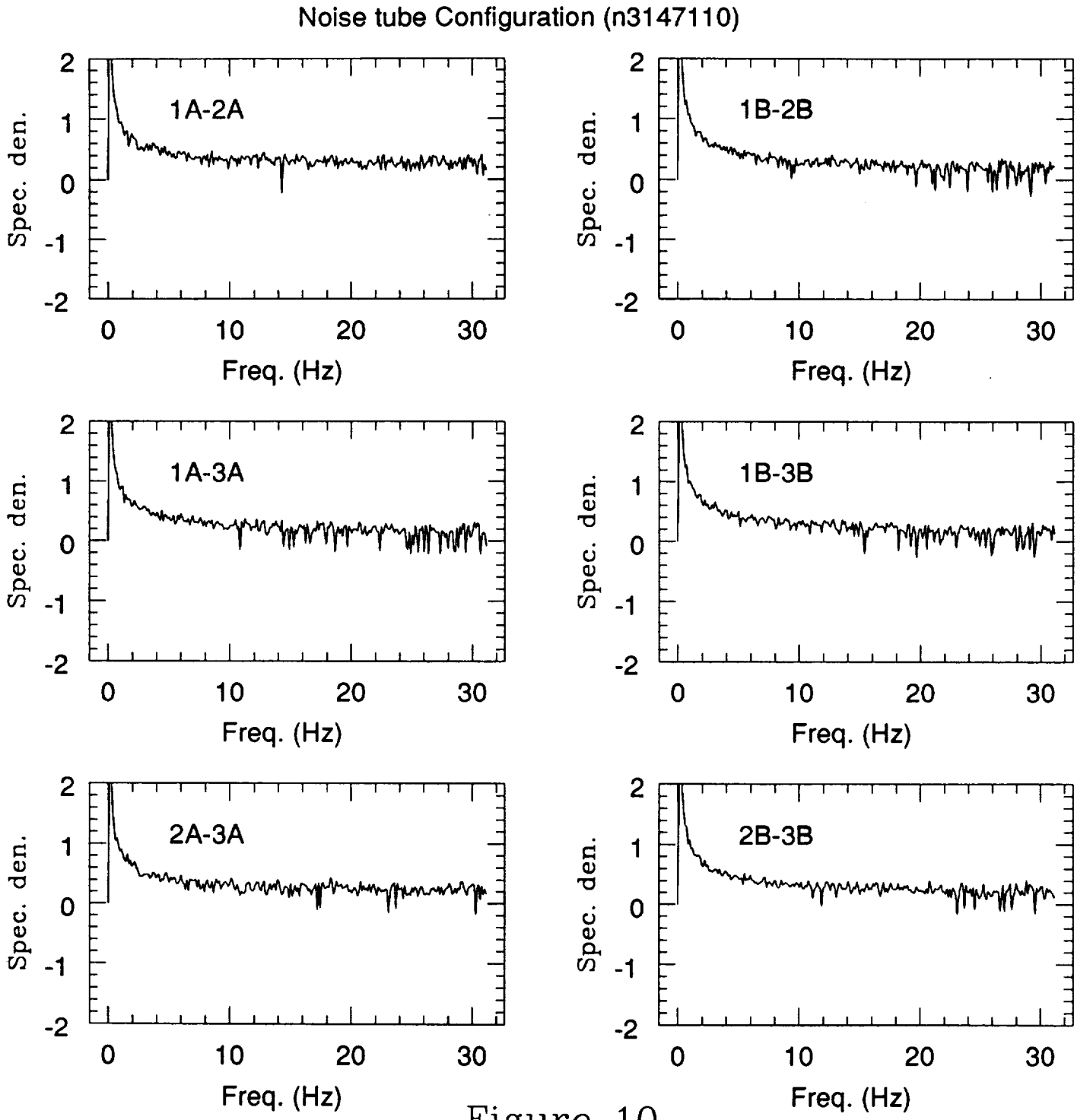
Noise tube Configuration (n3147110)
1A-2A
1B-2B
1A-3A
1B-3B
2A-3A
2B-3B
Spec. den.
Freq. (Hz)
2
1
0
-1
-2
0
10
20
30

Figure 10

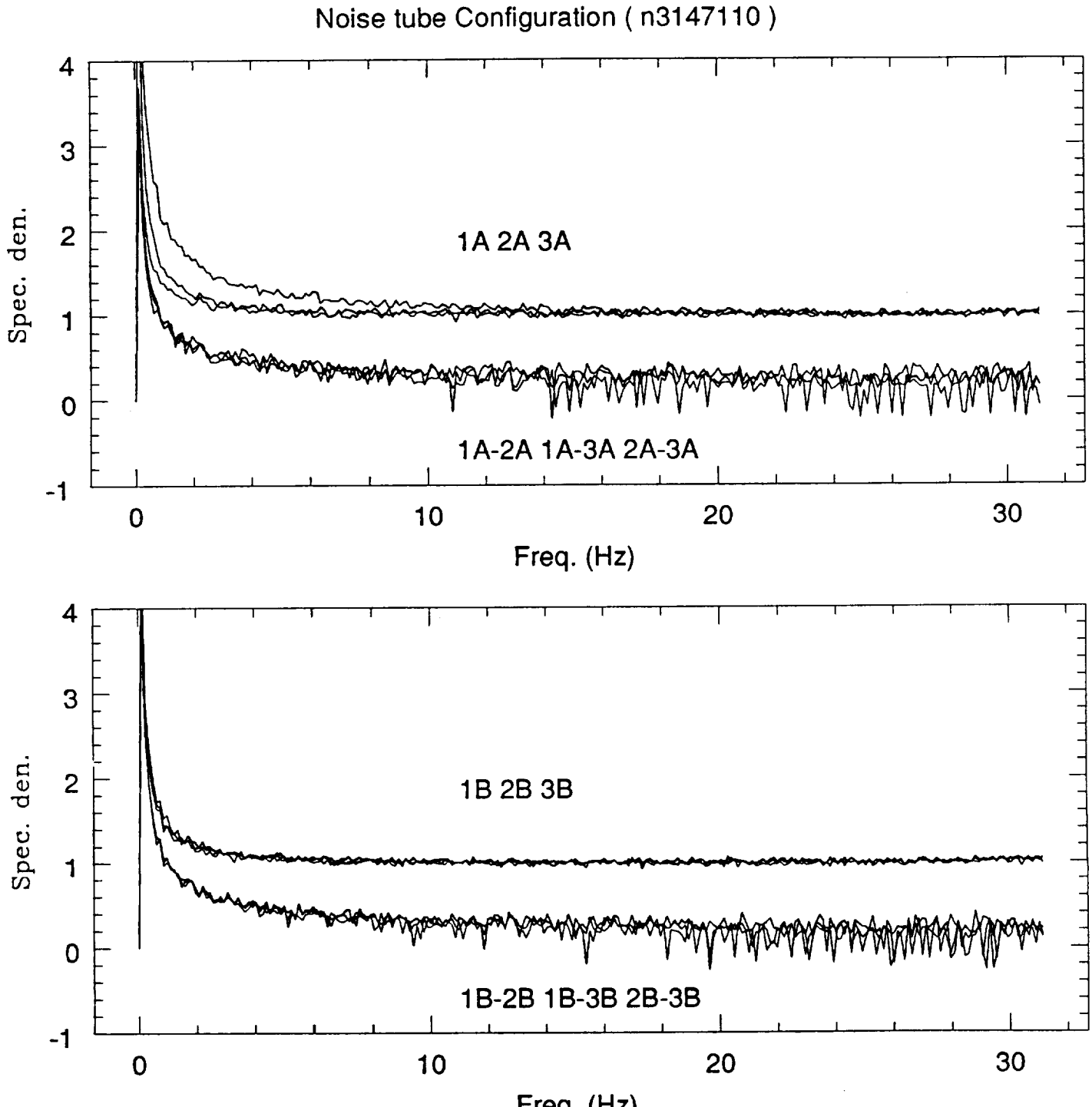
Noise tube Configuration (n3147110)
Spec. den.
4
3
2
1
0
-1
1A 2A 3A
1A-2A 1A-3A 2A-3A
0
10
20
30
Freq. (Hz)
Spec. den.
4
3
2
1
0
-1
1B 2B 3B
1B-2B 1B-3B 2B-3B
0
10
20
30
Freq. (Hz)

Figure 11

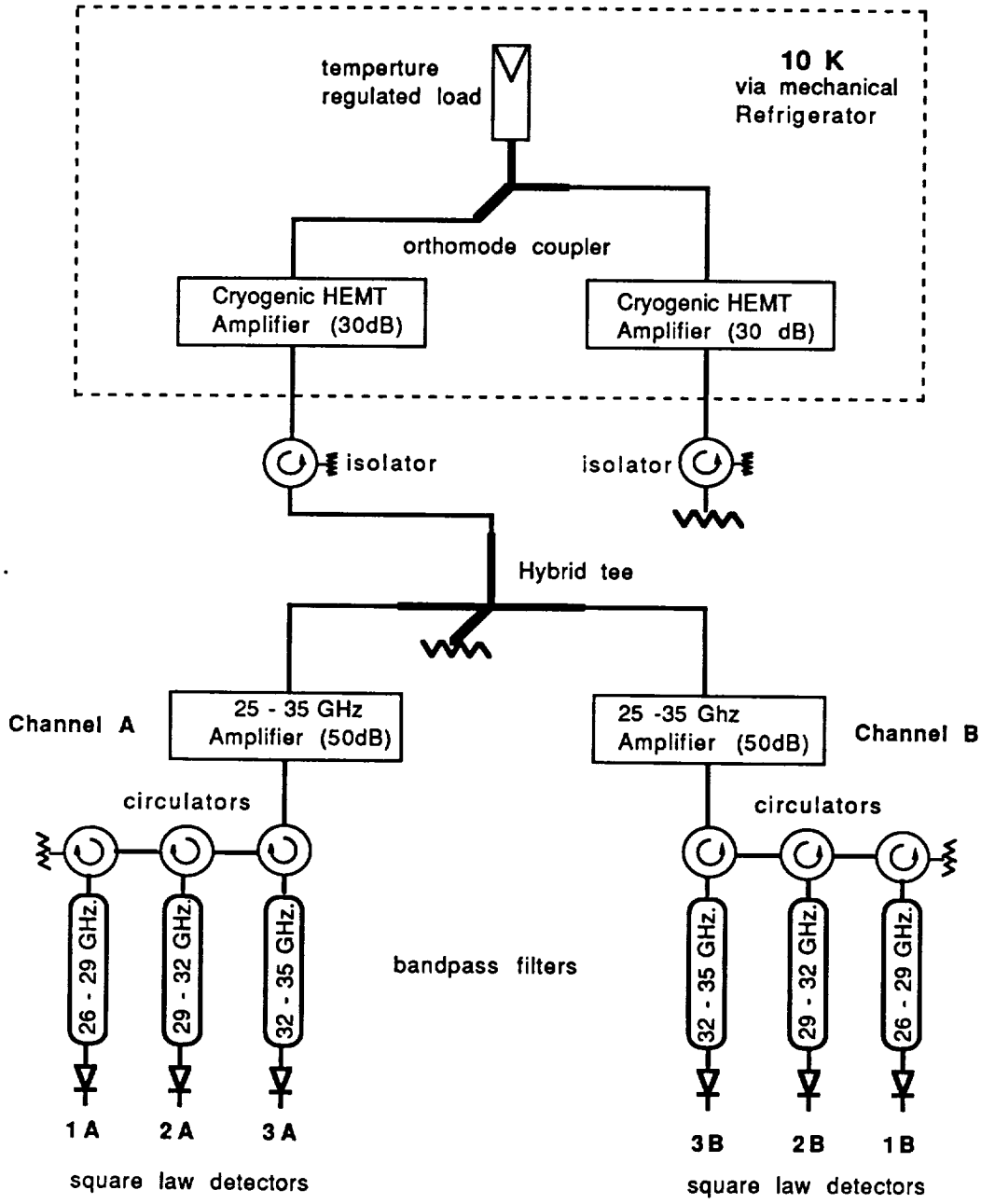
temperture
regulated load
10 K
via mechanical
Refrigerator
orthomode coupler
Cryogenic HEMT
Amplifier (30dB)
Cryogenic HEMT
Amplifier (30 dB)
isolator
isolator
Hybrid tee
Channel A
25 - 35 GHz
Amplifier (50dB)
25 -35 Ghz
Amplifier (50dB)
Channel B
circulators
circulators
26 - 29 GHz.
29 - 32 GHz.
32 - 35 GHz.
bandpass filters
32 - 35 GHz.
29 - 32 GHz.
26 - 29 GHz.
1 A
2 A
3 A
3B
2B
1B
square law detectors
square law detectors

Figure 12

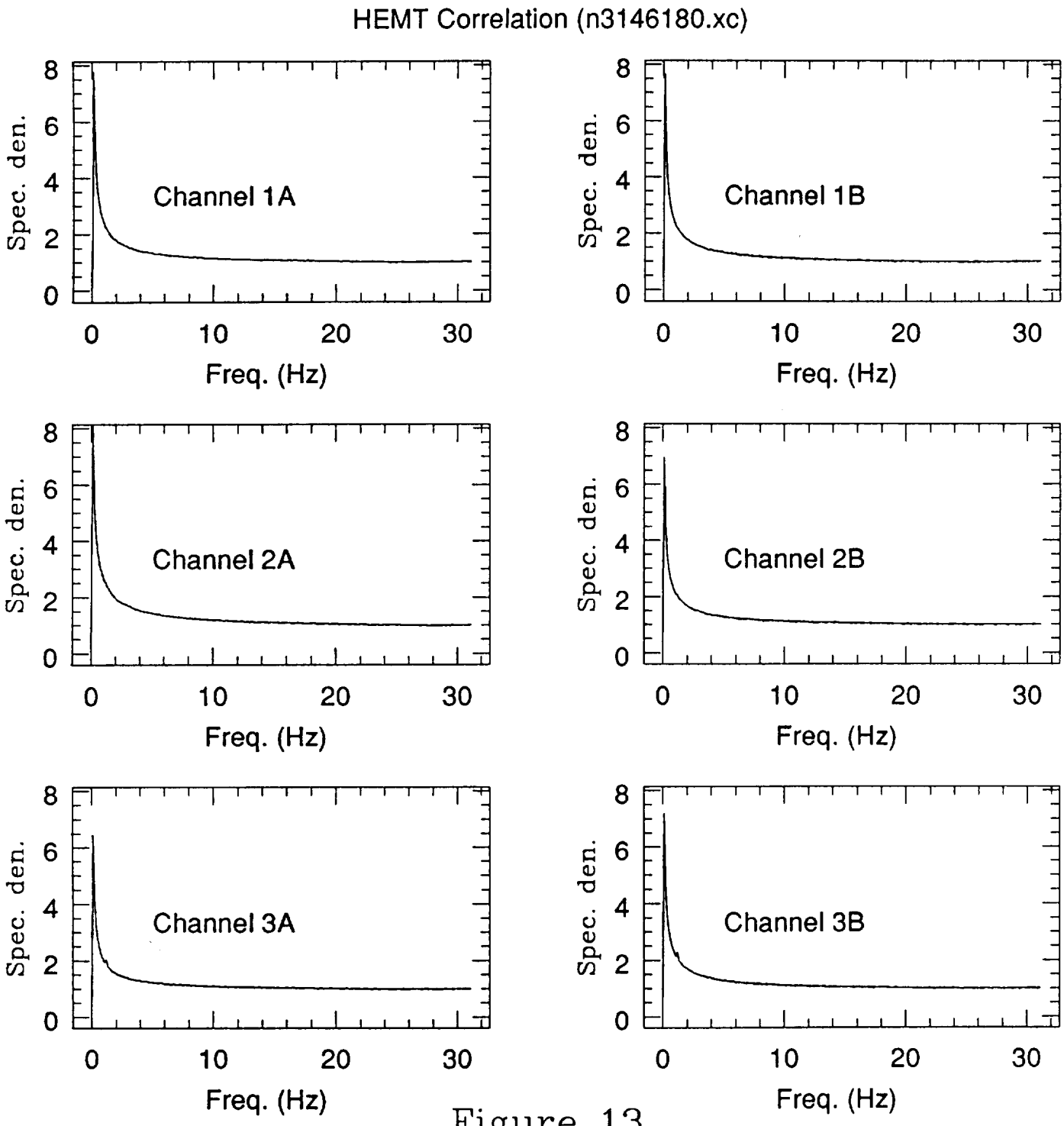
HEMT Correlation (n3146180.xc)
Channel 1A
Channel 1B
Channel 2A
Channel 2B
Channel 3A
Channel 3B
Spec. den.
Freq. (Hz)
0
2
4
6
8
0
10
20
30

Figure 13

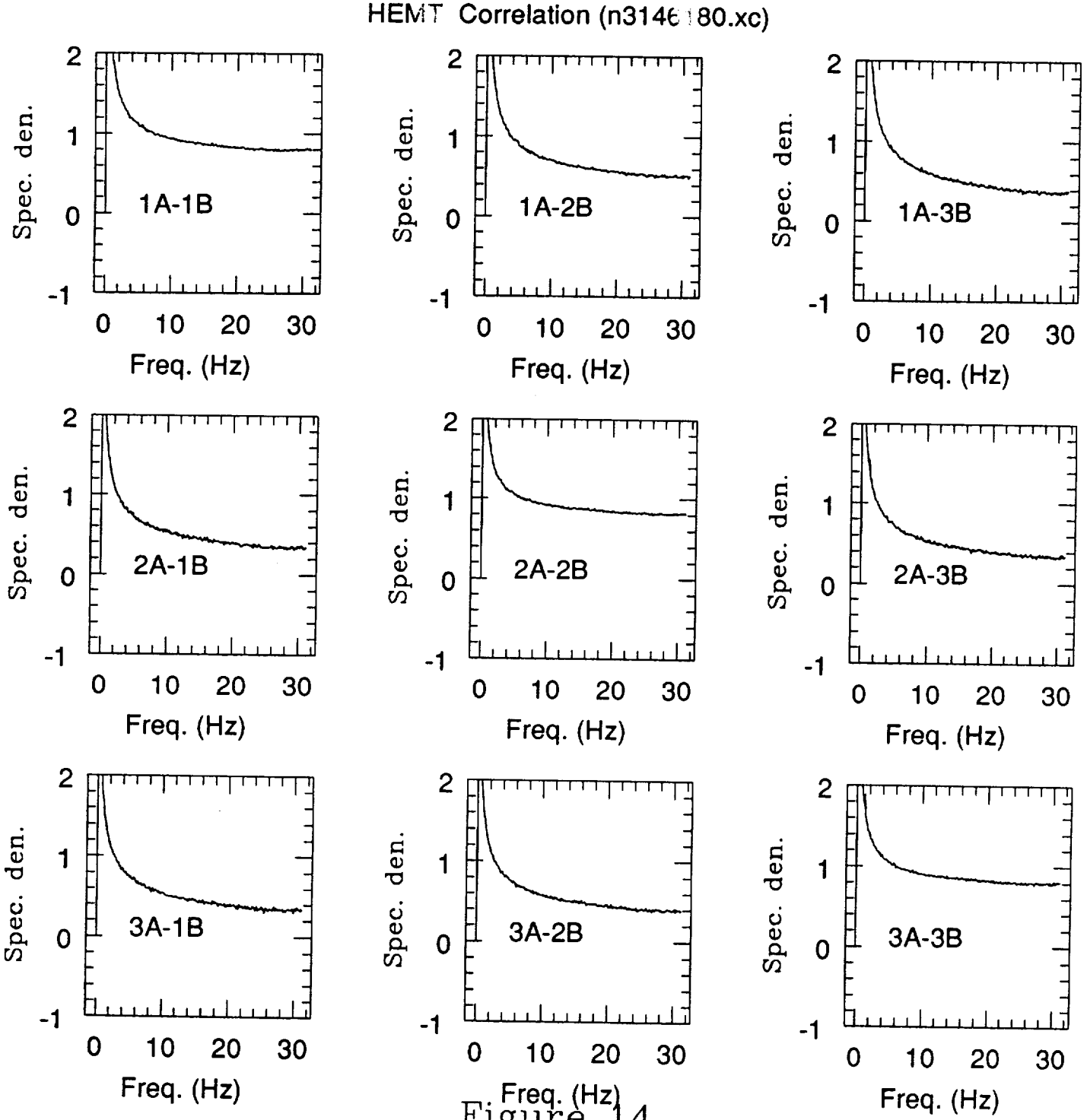
HEMT Correlation (n3146180.xc)
Spec. den.
Freq. (Hz)
1A-1B
1A-2B
1A-3B
2A-1B
2A-2B
2A-3B
3A-1B
3A-2B
3A-3B
2
1
0
-1
0
10
20
30

Figure 14

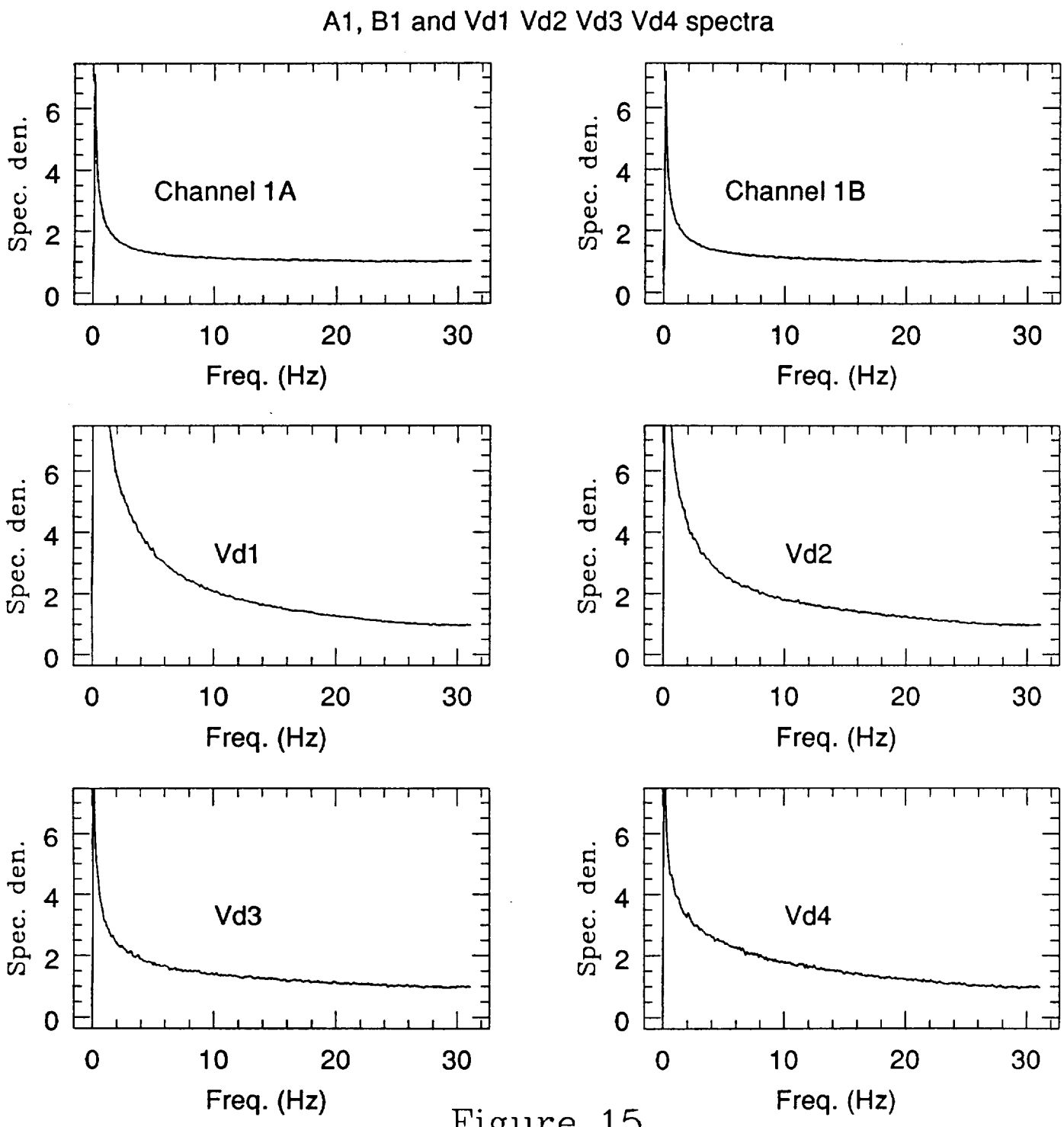
A1, B1 and Vd1 Vd2 Vd3 Vd4 spectra
Channel 1A
Channel 1B
Vd1
Vd2
Vd3
Vd4
Spec. den.
Freq. (Hz)
0
2
4
6
0
10
20
30

Figure 15

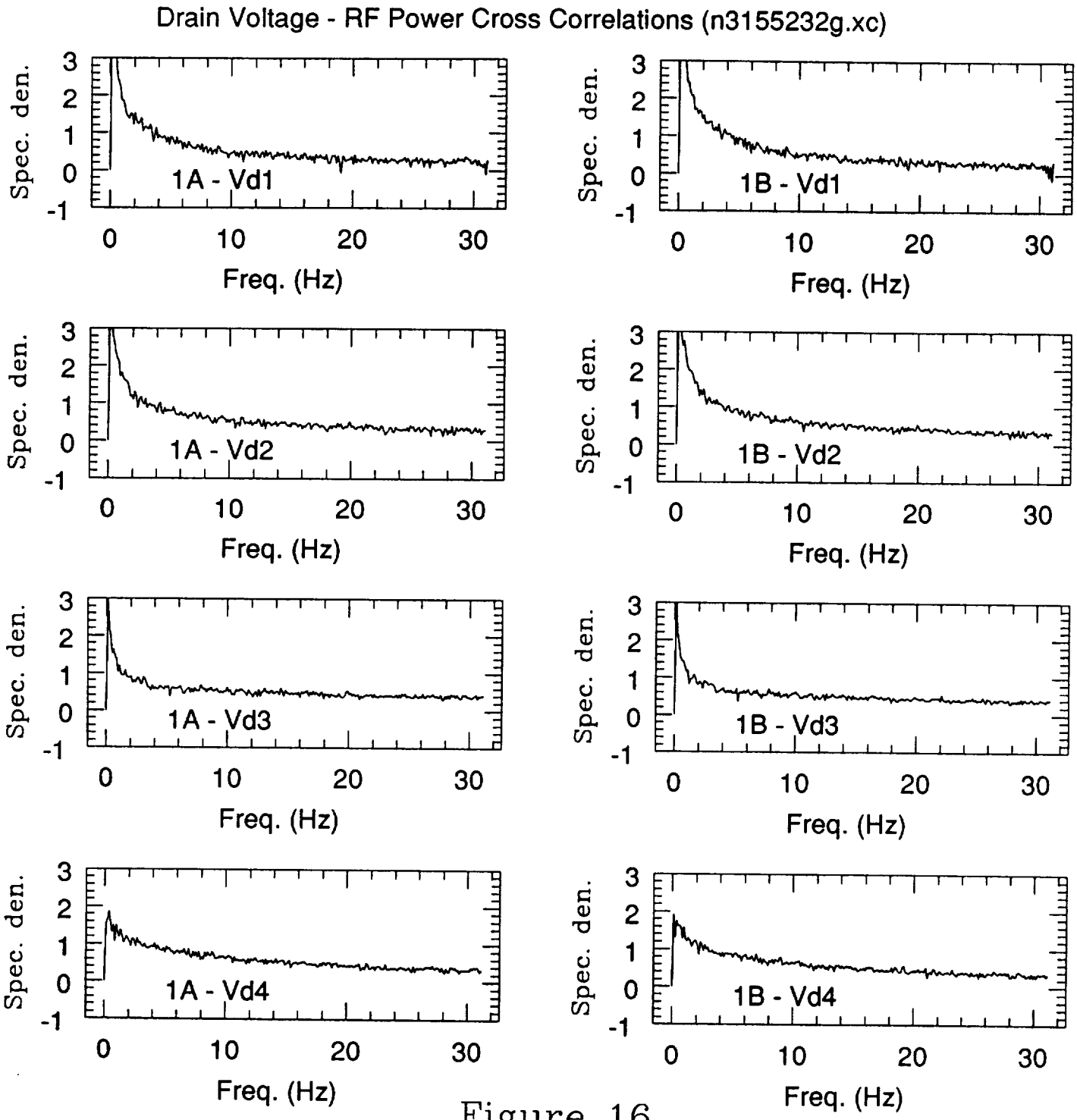
Drain Voltage - RF Power Cross Correlations (n3155232g.xc)
Spec. den.
Freq. (Hz)
1A - Vd1
1B - Vd1
1A - Vd2
1B - Vd2
1A - Vd3
1B - Vd3
1A - Vd4
1B - Vd4

Figure 16

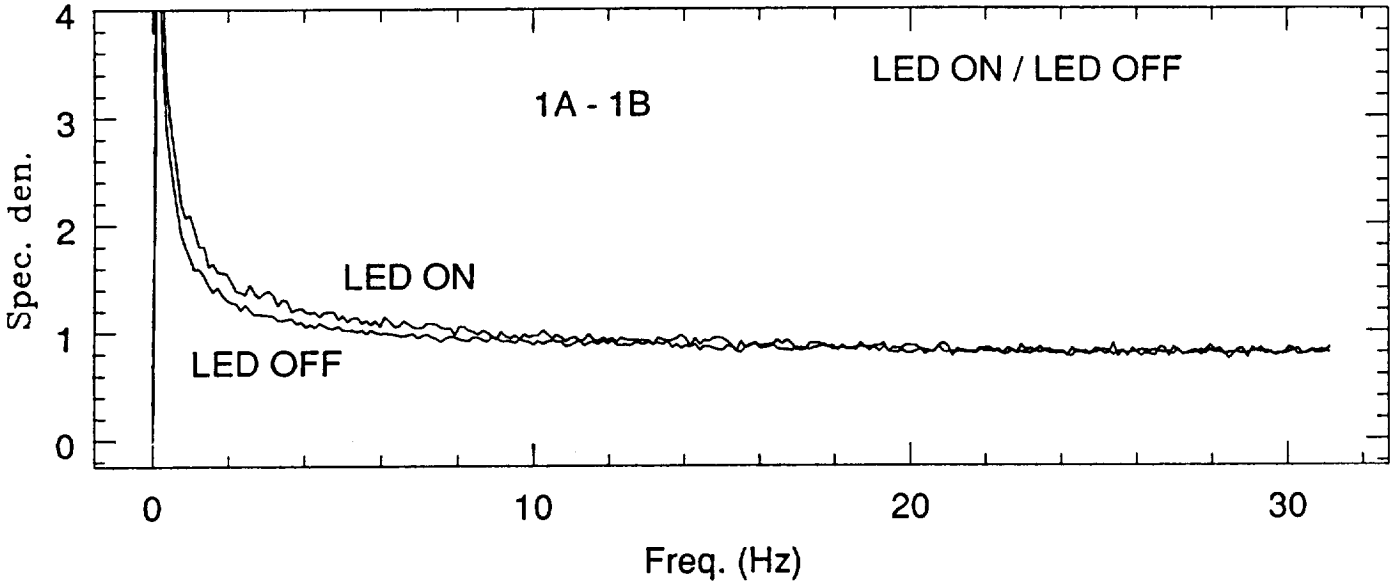

Figure 17

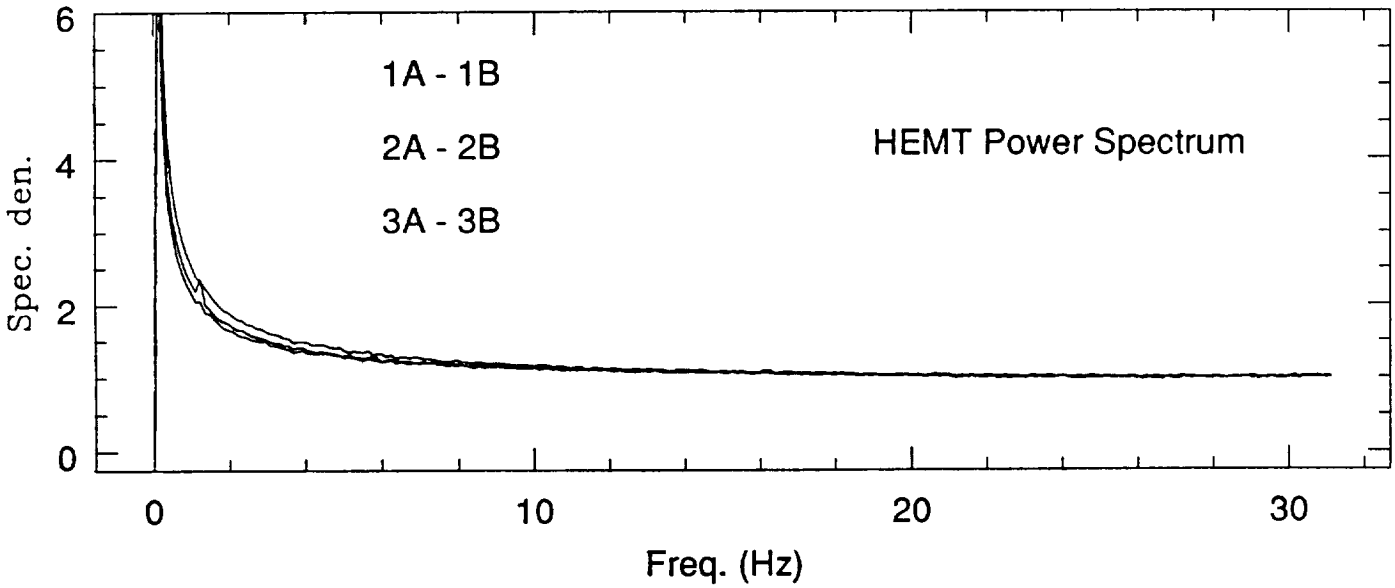

Figure 18

Frequency (Hz)	Noise Spectral Density ($K/\sqrt{Hz}$)
0.1221	8.427
0.2441	5.450
0.3662	4.173
0.4883	3.589
0.6104	3.212
0.7324	2.925
0.8545	2.719
0.9766	2.559
1.099	2.398
2.075	1.855
3.052	1.611
4.028	1.485
5.005	1.372
5.981	1.328
7.080	1.262
8.057	1.222
9.033	1.204
10.01	1.160
12.08	1.133
14.04	1.108
15.99	1.061
18.07	1.058
20.02	1.038
21.97	1.014
24.05	1.009
25.02	1.007
30.03	1.012

Table 1: Tabulated power spectral density of fluctuations at the output port of a HEMT amplifier with the amplifier's input attached to a 15 K temperature-regulated load. The results are normalized to unity above 25 Hz as described in the text.